

## Supporting Information

### **MOF-templated nitrogen-doped porous carbon materials as efficient electrocatalysts for oxygen reduction reaction**

Suhong Wang,<sup>a†</sup> Lin Liu,<sup>a†</sup> Shi-Ming Wang,<sup>b\*</sup> Zhengbo Han<sup>a\*</sup>

a. College of Chemistry, Liaoning University, Shenyang 110036, People's Republic of China.  
E-mail: ceshzb@lnu.edu.cn

b. College of Light Industry, Liaoning University, Shenyang 110036, People's Republic of China. E-mail: wangsm383@163.com

† The two authors contributed equally to this paper.

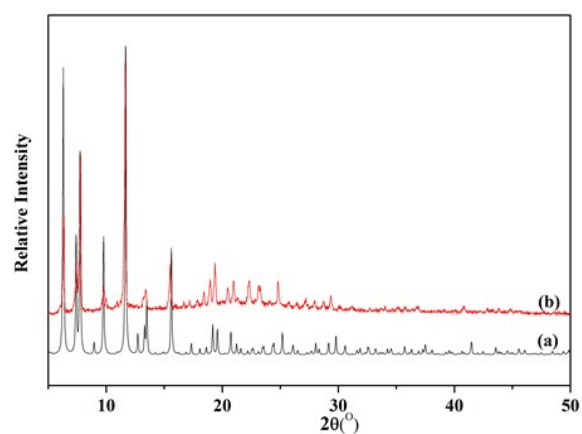


**Figure S1.** The simulated (a) and experimental (b) PXRD profiles of  $[(\text{CH}_3)_2\text{NH}_2]_6[\text{Ni}(\text{H}_2\text{O})_6]_3\{\text{Ni}_6(\eta^6\text{-TATAT})_4(\text{H}_2\text{O})_{12}\} \cdot 11\text{H}_2\text{O}$ .

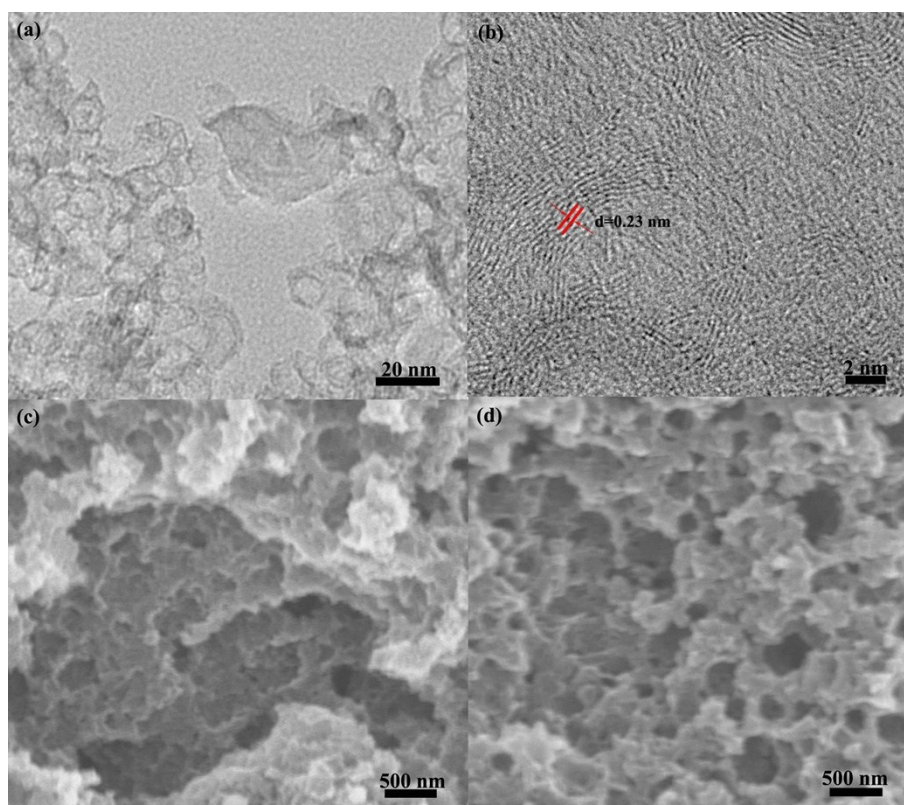


**Figure S2.** The TEM (a), HRTEM (b) and SEM (c and d) of NPC-800.

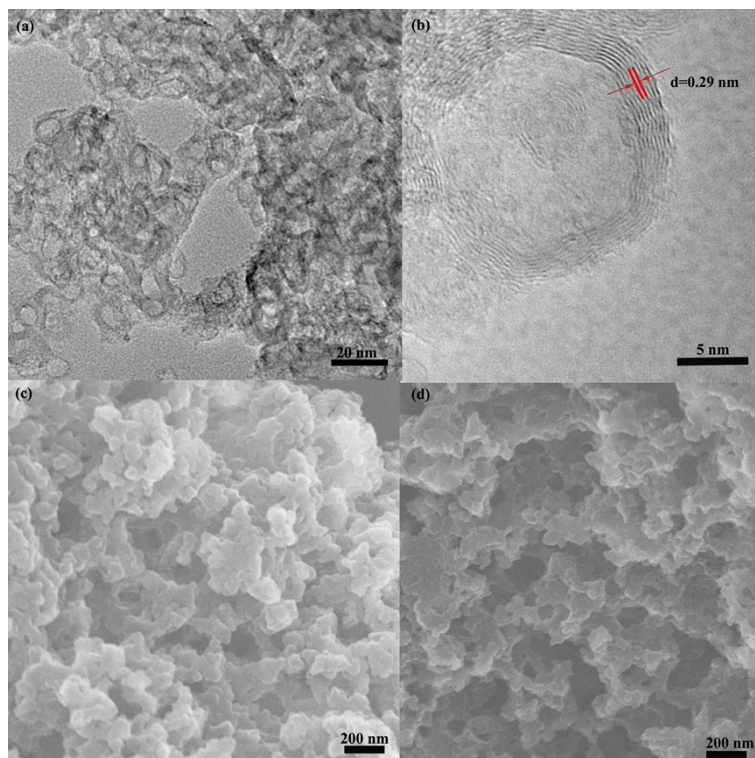


**Figure S3.** The TEM (a), HRTEM (b) images NPC-1000 and SEM (c and d) of NPC-1000.

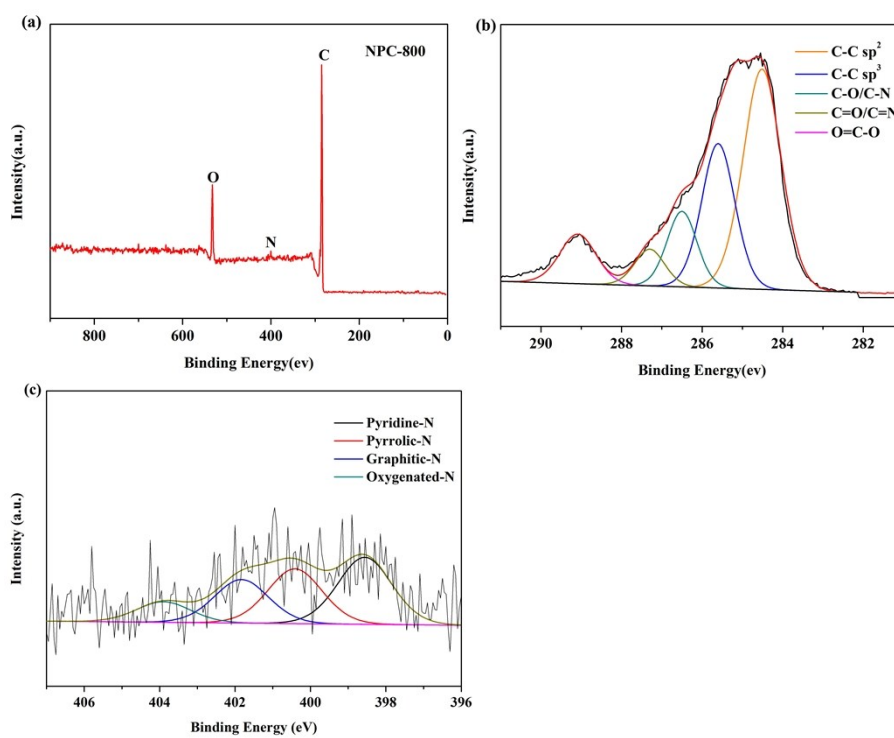


**Figure S4.** Typical survey scan XPS spectrum (a), deconvoluted C1s spectrum (b) and deconvoluted N1s spectrum (c) of NPC-800.

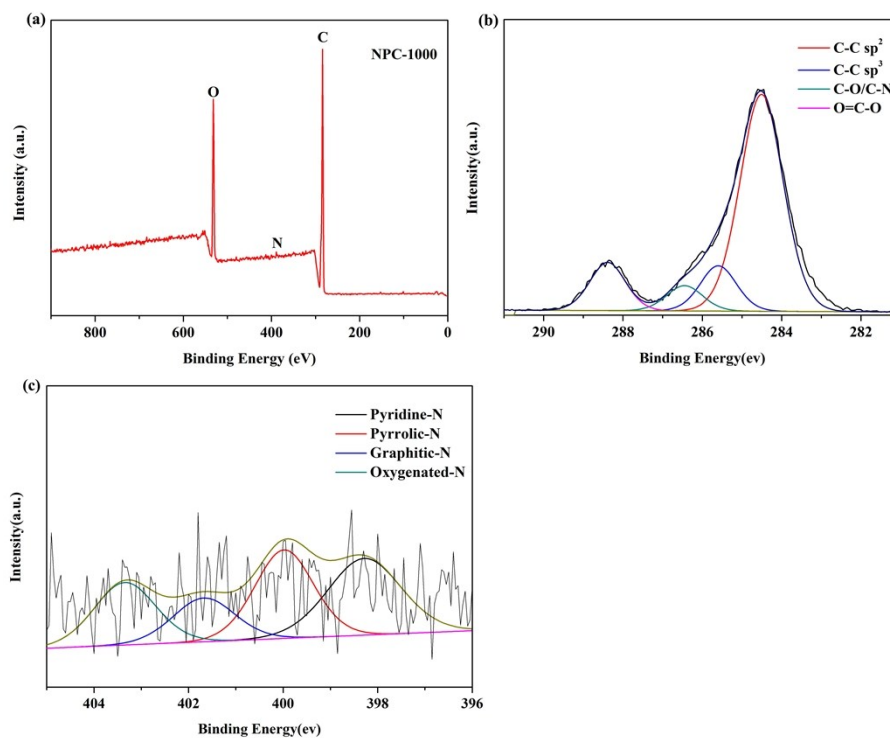


**Figure S5.** Typical survey scan XPS spectrum (a), deconvoluted C1s spectrum (b) and deconvoluted N1s spectrum (c) of NPC-1000.

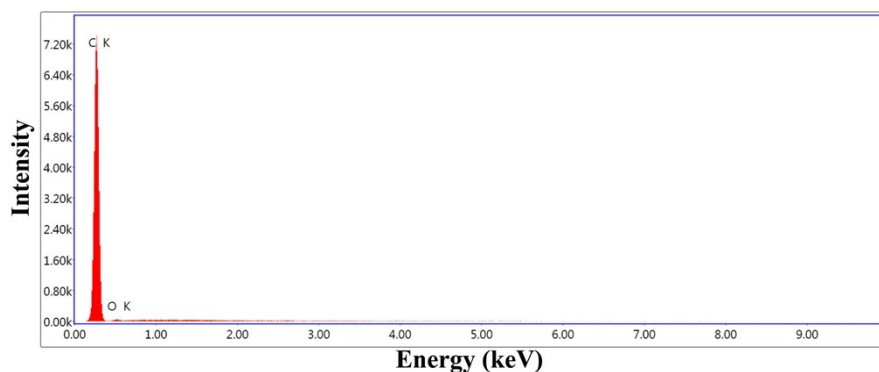


**Figure S6.** The EDS analysis of the carbonized MOF. The content of C is 97.64%, the content of O is 2.36%.

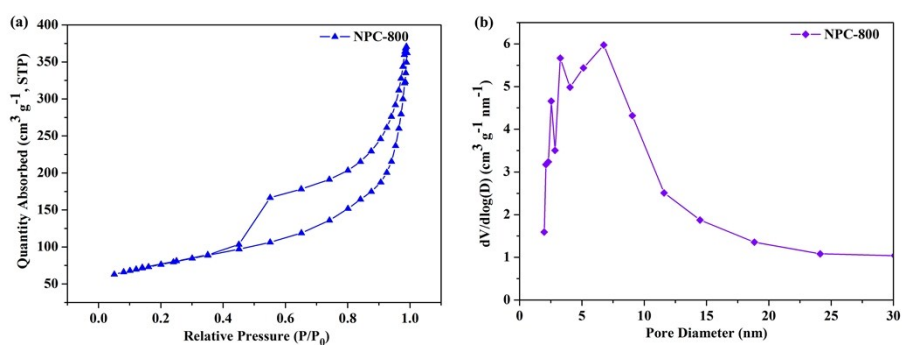


**Figure S7.** Nitrogen adsorption–desorption isotherm of NPC-800 (a), the

corresponding pore diameter distribution (b).

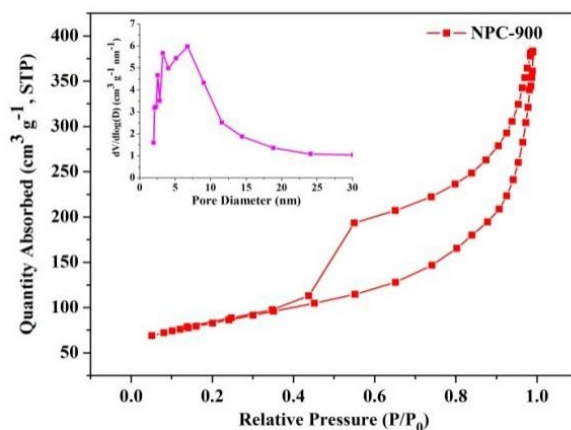


**Figure S8.** Nitrogen adsorption-desorption isotherm of NPC-900 (inset: the corresponding pore diameter distribution).

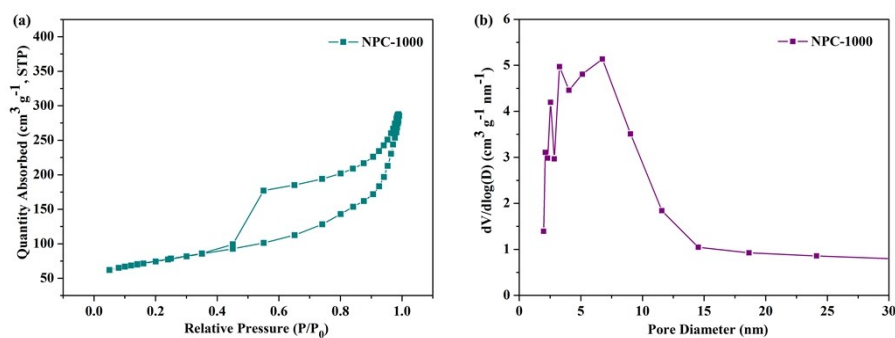


**Figure S9.** Nitrogen adsorption-desorption isotherm of NPC-1000 (a), the corresponding pore diameter distribution (b).

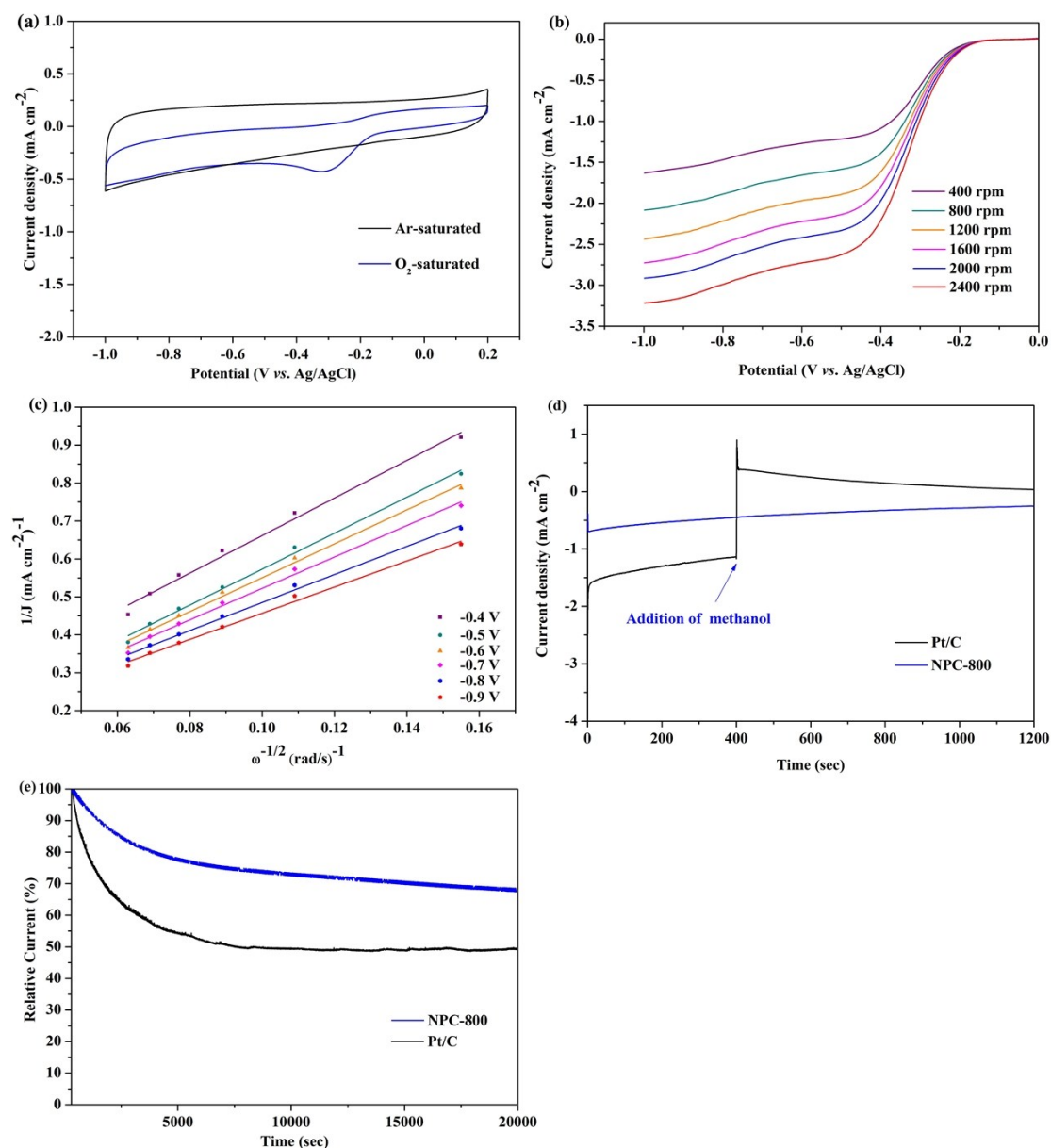


**Figure S10.** (a) CVs of the NPC-800 catalyst in O<sub>2</sub>-saturated (blue line) or Ar-saturated (black line) 0.1 M KOH at a scan rate of 50 mV s<sup>-1</sup>. (b) LSV of NPC-800 in O<sub>2</sub>-saturated 0.1 M KOH with a sweep rate of 10 mV s<sup>-1</sup> at the different rotation rates indicated. (c) Koutechy–Levich plots of NPC-800 at various potentials. (d) Chronoamperometric responses of NPC-800 and 20 wt% Pt/C upon addition of 3 M methanol into O<sub>2</sub>-saturated 0.1 M KOH at -0.2 V. (e) Stability evaluation of Pt/C (black) and NPC-800 (blue) in O<sub>2</sub>-saturated 0.1 M KOH at -0.2 V and rotation speed of 1600 rpm.

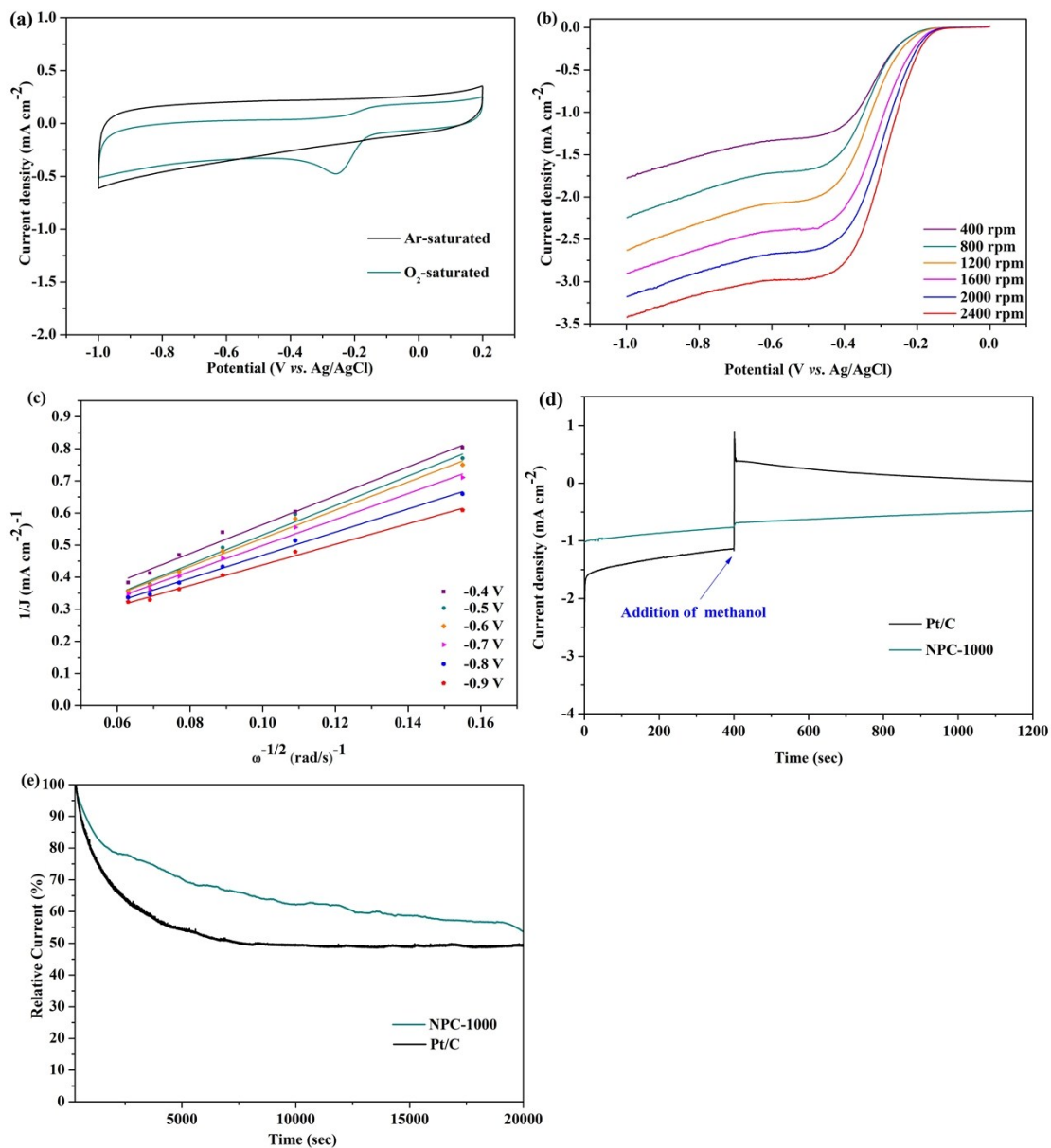


**Figure S11.** (a) CVs of ORR on the NPC-1000 catalyst in O<sub>2</sub>-saturated (green line) or Ar-saturated (black line) 0.1 M KOH at a scan rate of 50 mV s<sup>-1</sup>. (b) NPC-1000 in O<sub>2</sub>-saturated 0.1 M KOH with a sweep rate of 10 mV s<sup>-1</sup> at the different rotation rates indicated. (c) Koutechy–Levich plots of NPC-1000 at various potentials. (d) Chronoamperometric responses of NPC-1000 and 20 wt% Pt/C upon addition of 3 M methanol into O<sub>2</sub>-saturated 0.1 M KOH at -0.2 V. (e) Stability evaluation of Pt/C (black) and NPC-1000 (green) in O<sub>2</sub>-saturated 0.1 M KOH at -0.2 V and rotation speed of 1600 rpm.

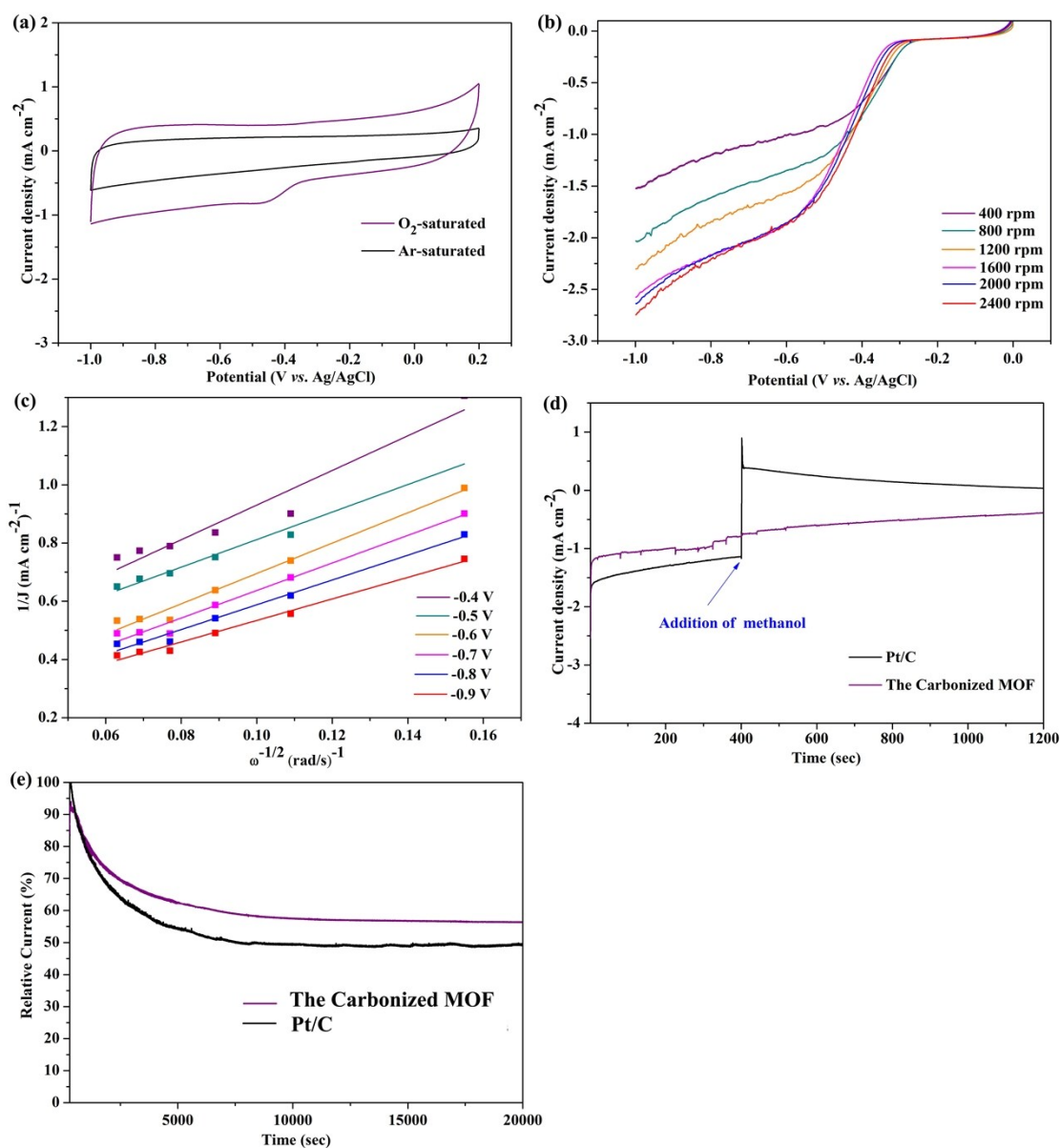


**Figure S12.** (a) CVs of ORR on the carbonized MOF catalyst in  $O_2$ -saturated (purple line) or Ar-saturated (black line) 0.1 M KOH at a scan rate of  $50 \text{ mV s}^{-1}$ . (b) the carbonized MOF in  $O_2$ -saturated 0.1 M KOH with a sweep rate of  $10 \text{ mV s}^{-1}$  at the different rotation rates indicated. (c) Koutechy–Levich plots of the carbonized MOF at various potentials. (d) Chronoamperometric responses of the carbonized MOF and 20 wt% Pt/C upon addition of 3 M methanol into  $O_2$ -saturated 0.1 M KOH at  $-0.2 \text{ V}$ . (e) Stability evaluation of Pt/C (black) and the carbonized MOF (purple) in  $O_2$ -saturated 0.1 M KOH at  $-0.2 \text{ V}$  and rotation speed of 1600 rpm.